# Nodeless Bulk Superconductivity in the Time-Reversal Symmetry Breaking Bi/Ni Bilayer System

Prashant Chauhan,[1] Fahad Mahmood,[1,*] Di Yue,[2] Peng-Chao Xu,[2] Xiaofeng Jin,[2] and N. P. Armitage[1,†]
[1]The Institute for Quantum Matter, Department of Physics and Astronomy, The Johns Hopkins University, Baltimore, Maryland 21218, USA
[2]Department of Physics, Fudan University, Shanghai 200433, China

(Received 17 September 2018; published 9 January 2019)

Epitaxial bilayer films of Bi(110) and Ni host a time-reversal symmetry breaking superconducting order with an unexpectedly high transition temperature $T_c = 4.1$ K. Using time-domain THz spectroscopy, we measure the low energy electrodynamic response of a Bi/Ni bilayer thin film from 0.2 to 2 THz as a function of temperature and magnetic field. We analyze the data in the context of a Bardeen-Cooper-Schrieffer-like superconductor with a finite normal-state scattering rate. In a zero magnetic field, all states in the film become fully gapped, providing important constraints into possible pairing symmetries. Our data appear to rule out the odd-frequency pairing that is natural for many ferromagnetic-superconductor interfaces. By analyzing the magnetic field-dependent response in terms of a pair-breaking parameter, we determine that superconductivity develops over the entire bilayer sample which may point to the $p$-wave like nature of unconventional superconductivity.

DOI: 10.1103/PhysRevLett.122.017002

Unconventional superconductors that break time-reversal symmetry (TRS) are promising platforms to realize Majorana edge modes. A remarkable candidate is a Bi(110) thin film deposited on a ferromagnetic Ni layer. This Bi/Ni bilayer system can have a $T_c$ as high as 4.1 K [1,2], which is quite unexpected for a number of reasons. Elemental bismuth (Bi) has a high atomic mass and low Fermi energy, factors which generally preclude superconductivity according to standard Bardeen-Cooper-Schrieffer (BCS) theory. Similarly, Ni is not superconducting at any temperature and, within conventional models of superconductivity, its ferromagnetism should inhibit rather than enhance superconductivity in the adjoining Bi layer [3,4].

With advances in epitaxial film growth and developments in topological and TRS breaking superconductivity, there has been renewed interest in this Bi/Ni bilayer system [5–10]. Two key results include the observation of a zero-bias anomaly in point-contact Andreev reflection [6], a possible indicator of Majorana modes, and broken TRS as determined by polar Kerr effect measurements [5]. TRS breaking suggests a complex pairing symmetry such that the phase of the superconducting order parameter winds around the Fermi surface. Examples of complex pairing include $d_{xy} \pm id_{x^2-y^2}$, which corresponds to even parity pairing, and $p_x \pm ip_y$, which consists of odd parity pairing. Because this system is noncentrosymmetric and has large spin-orbit coupling, the superconducting order may be a novel pairing state with a mixture of even and odd parity components [11,12].

There are two natural questions associated with the unconventional superconductivity in this system: (1) what is the gap structure of the superconducting order and does it have nodes or not? And (2) what is the mechanism for the superconductivity and where does it develop? Addressing these questions can have profound implications for the pairing symmetry in this system. For instance, it was proposed in Ref. [5] that this system exhibits $d_{xy} \pm id_{x^2-y^2}$ superconductivity because it is the lowest angular momentum state which is TRS violating, consistent with strong spin-orbit coupling and the approximate surface symmetries of this system. This proposal is based on superconductivity occurring on the Bi surface opposite to the Bi/Ni interface, as suggested by a systematic study of the thickness dependence of each of the Bi and Ni layers [6]. On the other hand, a few studies [13–15] suggest that superconductivity occurs in the bulk of the system (perhaps due to the presence of $s$-wave superconducting alloys such as $NiBi_3$ which may occur due to diffusion across the Bi/Ni interface). It was proposed recently [16] that this form of superconductivity combined with strong spin-orbit coupling of the Bi layer and the in-plane magnetic field of the Ni layer can lead to an effective $p_x \pm ip_y$ superconductivity instead of $d_{xy} \pm id_{x^2-y^2}$.

Here, we use time-domain THz spectroscopy (TDTS) to systematically study and track the superconducting gap as a function of both temperature and magnetic field. We find the gap is nodeless and can be described phenomenologically in terms of a weakly coupled BCS theory. Analysis of the field-dependent optical conductance points to superconductivity developing in the entire bilayer and not just the top surface. Moreover, from the calculation of the Fermi velocity of the superconducting charge carriers, it appears

 

that superconductivity does not develop in either the Bi or Ni electronic states independently.

A 10 nm thick rhombohedral Bi(110) layer was epitaxially grown on a 1 nm Ni(100) layer at 110 K, which is seeded on a 0.5 mm thick MgO(100) substrate at 300 K. TDTS measurements were performed on a total of three samples, each with the same $T_c$ of 4.15 K. They all gave similar results except for small differences at the lowest frequencies which may be due to differences in disorder levels. Both the real and imaginary parts of the complex conductance, $\tilde{G}(\omega)$, were obtained from the TDTS measurements, performed down to 1.6 K in both in-plane and out-of-plane magnetic fields.

Figures 1(a) and 1(b) show the temperature dependent $\tilde{G}(\omega)$ of the Bi/Ni bilayer between 0.2 and 2 THz at zero magnetic field. In the normal state (5 K), the real part of $\tilde{G}$, $G_1(\omega)$ shows a Drude-like Lorentzian peak feature, whereas the imaginary part $\tilde{G}_2(\omega)$ shows a positive dispersion corresponding to a finite scattering rate. We model the normal-state data using a Drude-Lorentz description for $\tilde{G}(\omega)$ [see Supplemental Material [17]]. From the fit, $G_1(\omega)$ in the limit $\omega \to 0$ is found to be 17.0 $\Omega^{-1}$, which matches quite well with the dc conductance measurement, $G_{dc} = 17.4\ \Omega^{-1}$ [see Supplemental Material [17]]. It is important to point out that the normal-state conductance of the bilayer is far larger than layers of just Bi(110) or Ni(001) individually [see Supplemental Material [17]] showing that the electronic structure of the bilayer is different than either of these materials. Below $T_c$, both $G_1(\omega)$ and $G_2(\omega)$ show features indicative of a fully gapped superconductor. As the temperature falls below $T_c$, a strong depletion develops in $G_1(\omega)$ [solid lines in Fig. 1(a)] at low $\omega$, corresponding to the opening up of the superconducting gap. The small $G_1(\omega)$ at subgap frequencies is due to the contribution of thermally excited quasiparticles, which becomes exponentially small as the temperature is lowered. Quite interestingly *all* metallic carriers appear to become gapped; within our experimental sensitivity there is no remnant metallic layer that does not go superconducting. This is also clear from a comparison of this data with the measured $G_1(\omega)$ of just Bi(110) and just Ni(001) individually [see Supplemental Material [17]]. $G_2(\omega)$ [Fig. 1(b)] increases as $\omega \to 0$ for $T < T_c$ and shows a $1/\omega$-like dependence at the lowest temperatures and frequencies, characteristic of the superconducting state.

To determine the superconducting gap $\Delta$, we simultaneously fit $G_1(\omega)$ and $G_2(\omega)$ using Mattis-Bardeen theory [26–28] for a uniformly gapped superconductor with a finite normal-state scattering rate [see Supplemental Material [17]] [29]. For the fitting procedure, the only free parameter is the superconducting gap, $\Delta(T)$, while the scattering rate and the plasma frequency are kept fixed to the values determined from the normal-state $G_1(\omega)$, as discussed above. The results of the fits are shown as dashed line in Figs. 1(a) and 1(b). The fit at the lowest temperature gives $\Delta(1.6\ \mathrm{K}) = 0.67$ meV, which is similar to the value obtained from tunneling spectroscopy (0.64 meV) [2]. The close agreement between the experimental data and Mattis-Bardeen fits indicates that the electrodynamic response of the Bi/Ni bilayer system below $T_c$ corresponds to that of a fully gapped superconductor. From the fitting, we obtain the zero temperature gap as $2\Delta(0) = 0.334$ THz (1.38 meV) or $2\Delta(0)/k_B T_c = 3.85$, i.e., very close to the weak coupling limit of 3.53 for a fully gapped BCS superconductor. The temperature evolution of the superconducting gap, $\Delta(T)$, [inset of Fig. 1(b)] closely follows the expected form for a BCS superconductor in the weak-coupling limit, as given by the standard numerical approximation $\Delta(T) = \Delta(0)\tanh[1.74\sqrt{T_c/T-1}]$ (black line). The observation of fully gapped superconductivity appears to rule out odd-frequency pairing that is natural for ferromagnetic-superconductor interfaces. Odd-frequency pairing is expected to have subgap spectral features [30–33]. Note that the $2\Delta/k_B T_c$ value we have observed is far less than the value of 12 observed in recent Andreev tunneling work [34].

To confirm the Mattis-Bardeen fits and get further insights into the superconducting gap structure, we study the temperature dependence of the superfluid spectral weight ($S_\delta$) as a direct measure of the superfluid density.

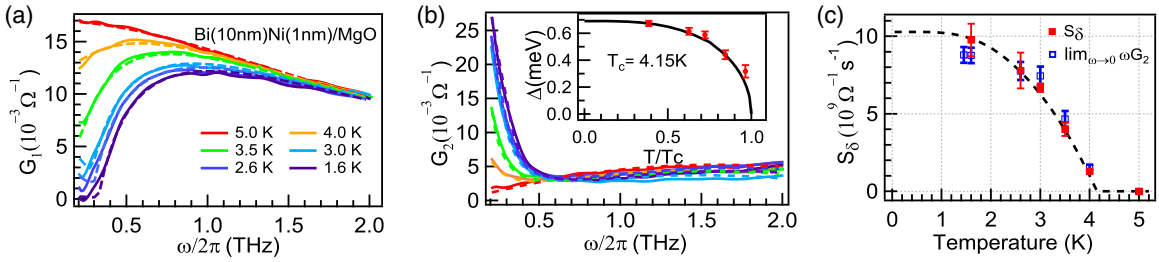


FIG. 1. (a) Real and (b) imaginary parts of the zero-field complex conductance of sample $A$ as a function of frequency from ($5\mathrm{K} > T_c$) to ($1.6\mathrm{K} \ll T_c$) with fits (dashed lines) to the data using Mattis-Bardeen theory for a BCS superconductor with a finite normal-state scattering rate. Inset: extracted temperature dependent energy gap with fit (solid line) to a BCS superconductor in the weak coupling limit. (c) Temperature dependent superfluid spectral weight, $S_\delta$. Red squares show the difference between the spectral weights of $G_1(\omega)$ at 5 K and various temperatures below $T_c$. Blue squares show $\lim_{\omega\to 0}\omega G_2$. The dashed line is the predicted superfluid spectral weight for a weakly coupled BCS superconductor. The error bars represent 2 standard deviations.

Using the Ferrel-Glover-Tinkham sum rule, $S_\delta$ can be extracted through $S_\delta = S_n - S_{qp}$, where $S_n$, the total spectral weight, is determined by the area under the $G_1(\omega)$ curve for the normal-state Drude conductance at 5 K and $S_{qp}$, the quasiparticle spectral weight, is the area under the $G_1(\omega)$ curve for temperatures below $T_c$. It can be seen in Fig. 1(c), the temperature evolution of $S_\delta(T)$ extracted using this method follows the predicted behavior of a fully gapped BCS superconductor (dashed black line), as given by $S_\delta(T) = [S_\delta(0)\Delta(T)/\Delta(0)]\tanh[\Delta(T)/2k_BT]$ [35]. An independent way to extract $S_\delta$ from our TDTS measurements, without relying on any fits, is through the limit $S_\delta = \lim_{\omega\to 0}\omega G_2$. We linearly extrapolate the measured $\omega G_2(\omega)$ down to $\omega = 0$ [see Supplemental Material [17] ] and plot it on Fig. 1(c) to compare the two methods of determining $S_\delta$. As can be seen, there is good agreement between the two that validates our overall fitting procedure.

The above analysis gives us important insights into the gap structure of the superconducting phase of Bi/Ni bilayer films. Some works [e.g., Ref. [6] ] suggested that this system has a complex $p$-wave type gap structure which is naturally compatible with the observed TRS breaking, similar to what is believed to be realized in $SrRu_2O_4$ [36,37]. Another possibility is complex $d$-wave pairing ($d_{xy} \pm id_{x^2-y^2}$), which is compatible with the surface crystal symmetry as argued by Gong *et al.* [5]. For these cases, the magnitude of the gap may be anisotropic and could lead to the observation of two energy gaps in the measurements of $G_1(\omega)$. However, our results on the Bi/Ni bilayer system closely correspond to those of a classic BCS weakly coupled superconductor with a uniform gap. If two $p$- or $d$-wave components do exist, then this implies that the system has an almost uniform gap structure with approximately equal magnitudes for each component [38–40]. Such low anisotropy [5] is consistent with the onset of superconductivity at a single transition temperature as observed.

We now use TDTS measurements in both in-plane and out-of-plane magnetic fields to understand where the superconductivity develops in the Bi/Ni bilayer system. Figures 2(a) and 2(b) show $G_1(\omega)$ and $G_2(\omega)$ for a few in-plane magnetic fields at $T = 1.6$ K [see Supplemental Material [17] for data at other fields]. The spectra show behavior similar to the zero-field temperature dependent spectra in Fig. 1(a); i.e., $G_1(\omega)$ approaches its normal-state behavior with increasing magnetic field while the gap size reduces. Similar to the analysis above, we fit $\tilde{G}(\omega)$ using Mattis-Bardeen theory with a single effective energy spectrum gap, $\Omega_G$ [dashed lines in Figs. 2(a) and 2(b)]. We obtain reasonable fits for most of the frequency range but note that a small amount of spectral weight at low frequencies on this sample $B$ is not captured by the fits. This discrepancy is discussed below as possibly originating from disorder in the films.

In general, the in-plane magnetic field results in pair breaking effects in the superconductor which leads to reduction in the pair-correlation gap $\Delta_p$. These effects can be quantified in terms of the Fermi velocity of the charge carriers through the behavior of the spectroscopic gap, $\Omega_G$, with field [Fig. 2(c)], as discussed below. This approach has also been applied for the electrodynamic response of Niobium Nitride thin films [41]. Here, $\Omega_G$ can be related to the pair correlation gap, $\Delta_p$, via the relation $\Omega_G = \Delta_p\{1 - [(4/\pi)\ln(\Delta_0/\Delta_p)]^{2/3}\}^{3/2}$ [42,43], where $\Delta_0$ is the zero-field energy gap at 1.6 K. The parameter $\Gamma$ that quantifies the strength of pair breaking can then be found using the relation $\ln[\Delta_p/\Delta_0] = -\pi\Gamma/4\Delta_p$ for $\Gamma < \Delta_p$ [42,44].

The extracted values of $\Omega_G$, $\Delta_p$, and $\Gamma$ as a function of in-plane field are shown in Fig. 2(c). For a thin film superconductor in an in-plane magnetic field, $\Gamma$ is expected to be proportional to the square of the magnetic field $H$ [35,41,42,44], which is indeed the case here [Fig. 2(c)]. An expression for $\Gamma$ in terms of the magnetic field is given by $\Gamma = bH^2 = D(eHd)^2/6$, where $d$ is the film thickness and $D = \tau_{tr}\nu_f^2/3$ is the diffusion constant for a charge carrier at the Fermi level in terms of the transport collision time $\tau_{tr}$ and the Fermi velocity $\nu_f$ [35,44]. By fitting the pair-breaking parameter $\Gamma$ to $bH^2$, we obtain $b = 0.0169(9)$ cm$^{-1}$/T$^2$. Using $\tau_{tr} = 47.5 \times 10^{-14}$ s as determined from the Drude fit to the normal state and the film

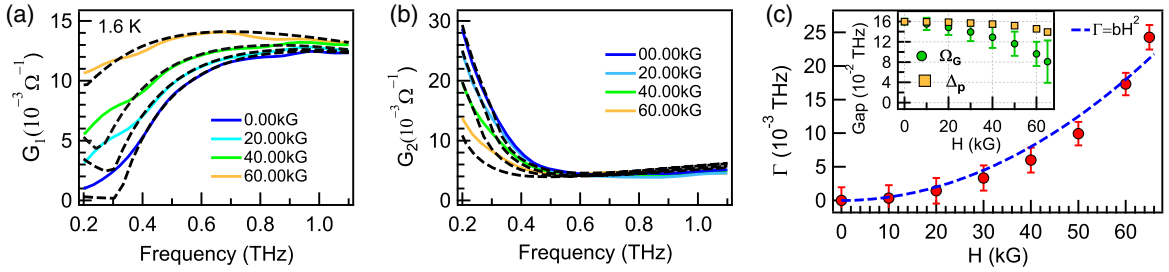


FIG. 2. (a),(b) In-plane field dependent real $G_1(\omega)$ and imaginary part $G_2(\omega)$ (solid lines) of the complex conductance for Bi/Ni bilayer sample $B$ at 1.6 K with fits (dashed lines) modeled using Mattis-Bardeen theory for an effective spectroscopic gap, $\Omega_G$. (c) Field dependence of pair-breaking parameter $\Gamma$, determined from optical conductance along with fit $\Gamma = bH^2$ (dashed line). Inset: the field dependence of $\Omega_G$ (green dots) and pair-correlation gap $\Delta_p$ (orange squares) for the Bi/Ni bilayer. The error bars represent the 95% confidence interval.

thickness $d = 11$ nm, we get $\nu_f = 0.201(20) \times 10^5$ m s$^{-1}$. This $\nu_f$ is much smaller than Fermi velocities of all the orientations of Bi and Ni crystals [see Supplemental Material [17] ]. This observation suggests that the superconducting quasiparticles do not belong to either of the individual components of the Bi/Ni bilayer separately. Note that in calculating $\nu_f$ we used the entire thickness of the Bi/Ni film ($d = 11$ nm). Although in principle the effective thickness could be much less, this choice is further justified by the out-of-plane magnetic field dependence described below.

In order to check the above determined value of $\nu_f$ without relying on the film thickness, we measure the optical response of the film to out-of-plane magnetic fields. In this case, the pair-breaking parameter is given by $\Gamma = DeH$ [35]. Figure 3(a) shows $G_1(\omega)$ for a number of out-of-plane magnetic fields at $T = 1.6$ K. Note that this system is a type II superconductor and so an out-of-plane magnetic field above $H_{c1} \sim 1.5$ kG forms vortices with normal metal cores. As the wavelength of the probing THz beam is much greater than the size of the vortex cores (∼nm), and is at high frequencies, the resulting electrodynamic response can be modeled in terms of the Maxwell-Garnett theory (MGT) [45] which is an effective medium theory. It has been applied to superconducting Niobium Nitride thin films by Xi *et al.* [46]. Within MGT, a superconducting thin film in an out-of-plane magnetic field is treated as a mixture of superconducting and normal metal components, where the superconducting component with volume fraction $(1 - f)$ is taken as the host medium and normal vortex cores with volume fraction $f$ as the embedded media [46]. We again use Mattis-Bardeen theory, similar to the in-plane field data, to describe the superconducting component and the Drude model to describe the normal metal cores [see Supplemental Material [17] for full details on MGT]. It is expected that due to the thin film geometry the magnetic field will almost uniformly penetrate the superconducting regions ($\Lambda_\perp = 2\lambda^2/d = 0.156$ mm).

The complex conductances for out-of-plane field dependent measurements are fit to the above described MGT using only $f$ and $\Omega_G$ as the free parameters. The resulting fits for $G_1(\omega)$ are shown as dashed lines in Fig. 3(a), whereas the extracted values for $f$ and $\Omega_G$ as a function of magnetic field are plotted in Fig. 3(b). The volume fraction $f$ is related to the applied field as $f \sim H/H_{c2}$ [46], where $H_{c2}$ is the upper critical field. As can be seen in Fig. 3(b), $f \propto H$ and a simple linear extrapolation to $f = 1$ yield $H_{c2} = 1.67 \pm 0.19$ T. This is in excellent agreement with the value of the upper critical field at 1.6 K determined from resistivity data (∼1.65 T) [7] and so justifies our analysis of the electrodynamic response in terms of MGT. Figure 3(c) shows the extracted values of $\Gamma$ as a function of field with a linear fit, $\Gamma = b_1 H$, (dashed line) giving $b_1 = 0.536(5)$ cm$^{-1}$/T$^2$. Using $b_1 = De$, we get $\nu_f = 0.201(3) \times 10^5$ m s$^{-1}$, which agrees with the value obtained from in-plane magnetic field data above. This confirms that the thickness of the superconducting film chosen in our earlier calculation is correct, and it appears the entirety of the bilayer film becomes superconducting.

Taken together with TRS breaking in the Bi/Ni bilayer, our observations of fully gapped superconductivity occurring in the bulk of the system rather than just on the surface seem to suggest an effective $p_x \pm ip_y$ pairing symmetry as proposed in Ref. [16]. Furthermore, given that above determined $\nu_f$ does not correspond to the Fermi-velocity of either Bi or Ni, and that the normal-state conductance of the bilayer is significantly higher than either of pure Bi or Ni [see Supplemental Material [17] ], it is indeed likely that superconductivity originates in new states that occur due to formation of the bilayer. Together with strong spin-orbit coupling from Bi and fluctuations from ferromagnetic Ni, this can lead to effective $p$-wave like superconductivity [16] It is not presently clear how our observation of a uniformly gapped superconductor can be reconciled with the recent report of an Anderson-Brinkman-Morel state using Andreev spectroscopy [34] since the Anderson-Brinkman-Morel state

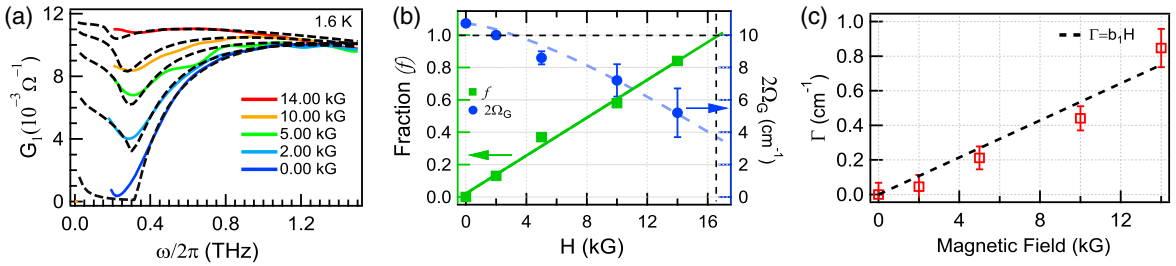


FIG. 3. (a) Out-of-plane field dependent real part, $G_1(\omega)$, (solid lines) of the complex conductance for Bi/Ni bilayer sample $C$ at 1.6 K. The dashed lines are fits obtained by modeling the response within Maxwell-Garnett theory, with the Drude model for the normal component and Mattis-Bardeen theory with effective spectroscopic gap $\Omega_G$ for the superconducting component. (b) Field dependent $\Omega_G$ (blue dots) and the normal-volume fraction $f$ (green squares) with fit $f = H/H_{c2}$ (solid line). The dashed blue line is a guide to the eye. Horizontal and vertical dashed lines represent $f = 1$ and $H_{c2}$, respectively. (c) Field dependent pair-breaking parameter $\Gamma$ fit to $\Gamma = bH$ (dashed line). The error bars represent the 95% confidence interval.

has a node along the $b$ direction. This deserves further investigation.

Finally, we would like to discuss the discrepancy between the in-plane field data in Figs. 2(a) and 2(b) and the Mattis-Bardeen type fits using a single gap. For a complex $p$- or $d$-wave order parameter, it is expected that an in-plane magnetic field may anisotropically suppress one of the order parameter components preferentially giving a pure single component at some transition field below $H_{c2}$ [e.g., Refs. [47,48] ]. This naturally results in low frequency absorption. It would be interesting to look for this transition field with other techniques such as heat capacity or nuclear magnetic resonance. Although the low frequency spectral weight we find may be reflective of this, another possibility is disorder in the films because they are highly susceptible to aging, air exposure, and imperfections during growth. This disorder could lead to low frequency absorption and thus the fits underestimate $\tilde{G}(\omega)$ [e.g., Refs. [49,50] ]. We note that we can get better fits when we introduce a small Gaussian distribution in the gap as shown in the Supplemental Material [17] (sec. VI), but these fits give roughly the same extracted parameters as above [see Supplemental Material [17–25] ]. Thus, a small amount of disorder in this fashion does not affect our overall conclusions.

Experiments at Johns Hopkins University were supported by the Army Research Office Grant No. W911NF-15-1-0560. Film growth at Fudan was supported by the National Basic Research Program of China (Grants No. 2015CB921402 and No. 2011CB921802) and the National Science Foundation of China (Grants No. 11374057, No. 11434003, and No. 11421404).

*fahad@jhu.edu
†npa@jhu.edu

[1] J. S. Moodera and R. Meservey, Phys. Rev. B **42**, 179 (1990).
[2] P. LeClair, J. S. Moodera, J. Philip, and D. Heiman, Phys. Rev. Lett. **94**, 037006 (2005).
[3] V. L. Ginzburg, J. Exp. Theor. Phys. **31**, 202 (1956).
[4] E. T. D. Saint-James and D. Sarma, *Type II Superconductivity* (Pergamon, New York, 1969).
[5] X. Gong, M. Kargarian, A. Stern, D. Yue, H. Zhou, X. Jin, V. M. Galitski, V. M. Yakovenko, and J. Xia, Sci. Adv. **3**, e1602579 (2017).
[6] G. Xin-Xin, Z. He-Xin, X. Peng-Chao, Y. Di, Z. Kai, J. Xiao-Feng, T. He, Z. Ge-Jian, and C. Ting-Yong, Chin. Phys. Lett. **32**, 067402 (2015).
[7] X.-X. Gong, H. Zhou, P.-C. Xu, D. Yue, K. Zhu, X. Jin, H. Tian, G. Zhao, and T.-Y. Chen, arXiv:1504.04232.
[8] H. Zhou, X. Gong, and X. Jin, J. Magn. Magn. Mater. **422**, 73 (2017).
[9] J. Wang, X. Gong, G. Yang, Z. Lyu, Y. Pang, G. Liu, Z. Ji, J. Fan, X. Jing, C. Yang, F. Qu, X. Jin, and L. Lu, Phys. Rev. B **96**, 054519 (2017).
[10] M. Keskin and N. arl, J. Magn. Magn. Mater. **437**, 1 (2017).
[11] E. Bauer and M. Sigrist, *Non-Centrosymmetric Superconductors*, Lecture Notes in Physics Vol. 847 (Springer, Berlin, Heidelberg, 2012).
[12] A. A. Schenck, *Muon Spin Rotation Spectroscopy: Principles and Applications in Solid State Physics* (A. Hilger, Bristol, England, 1985), p. 325.
[13] L. Y. Liu, Y. T. Xing, I. L. C. Merino, H. Micklitz, D. F. Franceschini, E. Baggio-Saitovitch, D. C. Bell, and I. G. Solórzano, Phys. Rev. Mater. **2**, 014601 (2018).
[14] V. Siva, K. Senapati, B. Satpati, S. Prusty, D. K. Avasthi, D. Kanjilal, and P. K. Sahoo, J. Appl. Phys. **117**, 083902 (2015).
[15] V. Siva, P. C. Pradhan, G. S. Babu, M. Nayak, P. K. Sahoo, and K. Senapati, J. Appl. Phys. **119**, 063902 (2016).
[16] S.-P. Chao, arXiv:1808.05333.
[17] See Supplemental Material at http://link.aps.org/supplemental/10.1103/PhysRevLett.122.017002, which includes Refs. [18–25], for details about the setup, MGT theory fits, and Fermi velocities of Bi and Ni.
[18] G. L. Carr, S. Perkowitz, and D. B. Tanner, *Infrared and Millimeter Waves* (Academic Press, Inc., New York, 1985), pp. 171–263.
[19] C. G. Granqvist and O. Hunderi, Phys. Rev. B **16**, 3513 (1977).
[20] A. Sihvola, J. Nanomater. **2007**, 1 (2007).
[21] C. Kirkegaard, T. K. Kim, and P. Hofmann, New J. Phys. **7**, 99 (2005).
[22] P. Hofmann, J. E. Gayone, G. Bihlmayer, Y. M. Koroteev, and E. V. Chulkov, Phys. Rev. B **71**, 195413 (2005).
[23] P. Hofmann, Prog. Surf. Sci. **81**, 191 (2006).
[24] N. Ashcroft and N. Mermin, *Solid State Physics*, 2nd ed. (Thomson Learning, Belmont, MA, 1976), p. 38.
[25] H. Ehrenreich, H. R. Philipp, and D. J. Olechna, Phys. Rev. **131**, 2469 (1963).
[26] D. C. Mattis and J. Bardeen, Phys. Rev. **111**, 412 (1958).
[27] M. Tinkham, Phys. Rev. **104**, 845 (1956).
[28] L. H. Palmer and M. Tinkham, Phys. Rev. **165**, 588 (1968).
[29] W. Zimmermann, E. Brandt, M. Bauer, E. Seider, and L. Genzel, Physica (Amsterdam) **183C**, 99 (1991).
[30] J. Linder, T. Yokoyama, A. Sudbø, and M. Eschrig, Phys. Rev. Lett. **102**, 107008 (2009).
[31] Y. Tanaka and A. A. Golubov, Phys. Rev. Lett. **98**, 037003 (2007).
[32] F. Bergeret, A. F. Volkov, and K. B. Efetov, Rev. Mod. Phys. **77**, 1321 (2005).
[33] A. Pal, J. A. Ouassou, M. Eschrig, J. Linder, and M. G. Blamire, Sci. Rep. **7**, 40604 (2017).
[34] G. J. Zhao, X. X. Gong, J. C. He, J. A. Gifford, H. X. Zhou, Y. Chen, X. F. Jin, C. L. Chien, T. Y. Chen, arXiv:1810.10403v1.
[35] M. Tinkham, *Introduction to Superconductivity: Second Edition* (Dover Publications, Mineola, N.Y., 2004), pp. 89–103.
[36] J. Xia, Y. Maeno, P. T. Beyersdorf, M. M. Fejer, and A. Kapitulnik, Phys. Rev. Lett. **97**, 167002 (2006).
[37] G. M. Luke, Y. Fudamoto, K. M. Kojima, M. I. Larkin, J. Merrin, B. Nachumi, Y. J. Uemura, Y. Maeno, Z. Q. Mao, Y. Mori, H. Nakamura, and M. Sigrist, Nature (London) **394**, 558 (1998).
[38] F. Loder, A. P. Kampf, and T. Kopp, Sci. Rep. **5**, 15302 (2015).

[39] M. Smidman, M. B. Salamon, H. Q. Yuan, and D. F. Agterberg, Rep. Prog. Phys. **80**, 036501 (2017).
[40] R. P. Singh, A. D. Hillier, B. Mazidian, J. Quintanilla, J. F. Annett, D. M. Paul, G. Balakrishnan, and M. R. Lees, Phys. Rev. Lett. **112**, 107002 (2014).
[41] X. Xi, J. Hwang, C. Martin, D. B. Tanner, and G. L. Carr, Phys. Rev. Lett. **105**, 257006 (2010).
[42] K. Maki, Prog. Theor. Phys. **31**, 731 (1964).
[43] S. Skalski, O. Betbeder-Matibet, and P. R. Weiss, Phys. Rev. **136**, A1500 (1964).
[44] R. D. Parks, *Superconductivity* (Marcel Dekker, Inc., New York, 1969), Vol. 2, pp. 1052, 1080, 1082.
[45] J. C. M. Garnett and J. LarmorPhilos. Trans. R. Soc. A **203**, 385 (1904).
[46] X. Xi, J.-H. Park, D. Graf, G. L. Carr, and D. B. Tanner, Phys. Rev. B **87**, 184503 (2013).
[47] D. F. Agterberg, Phys. Rev. Lett. **80**, 5184 (1998).
[48] Z. Q. Mao, Y. Maeno, S. NishiZaki, T. Akima, and T. Ishiguro, Phys. Rev. Lett. **84**, 991 (2000).
[49] B. Cheng, L. Wu, N. J. Laurita, H. Singh, M. Chand, P. Raychaudhuri, and N. P. Armitage, Phys. Rev. B **93**, 180511 (2016).
[50] M. Swanson, Y. L. Loh, M. Randeria, and N. Trivedi, Phys. Rev. X **4**, 021007 (2014).